Antigen Affinity Controls Rapid T-Dependent Antibody Production by Driving the Expansion Rather than the Differentiation or Extrafollicular Migration of Early Plasmablasts[1]

Tyani D. Chan,* Dominique Gatto,* Katherine Wood,* Tahra Camidge,* Antony Basten,* and Robert Brink[2]*†

To optimize the initial wave of Ab production against T-dependent Ags, primary B cell clones with the highest Ag affinity are selected to generate the largest extrafollicular plasmablast (PB) responses. The mechanism behind this remains undefined, primarily due to the difficulty of analyzing low frequency Ag-specific B cells during the earliest phases of the immune response when key differentiation decisions are made. In this study, a high resolution in vivo mouse model was used to characterize in detail the first 6 days of a T-dependent B cell response and to identify the steps at which initial Ag affinity has a major impact. Ag-specific B cells proliferated within splenic follicles from days 1.0 to 3.0 before undergoing a dynamic phase of multilineage differentiation (days 3.0–4.0) that generated switched and unswitched populations of germinal center B cells, early memory B cells, and extrafollicular PBs. PB differentiation was marked by synchronous up-regulation of CXCR4 and down-regulation of CXCR5 and the adoption of a unique BCR^{high} phenotype by unswitched PBs. Differences in Ag affinity of >50-fold did not markedly affect the early stages of the response, including the differentiation and extrafollicular migration of PBs. However, high affinity PBs underwent significantly greater expansion within the splenic bridging channels and red pulp, due to both increased proliferation and decreased apoptosis. Extrafollicular PBs maintained class II MHC, but not IL-21R expression, and interacted directly with Ag-specific extrafollicular Th cells, suggesting that IL-21-independent T cell help may drive extrafollicular PB expansion in responses to foreign Ag. *The Journal of Immunology,* **2009, 183: 3139–3149.**

Humoral immune responses against foreign T-dependent (TD)[3] Ags require collaboration between B lymphocytes (B cells) and CD4$^+$ T lymphocytes (Th cells) that recognize physically linked epitopes. Productive collaboration between Ag-specific B and T cells requires their colocalization to a defined environment within secondary lymphoid tissues. To achieve this, Ag-stimulated B cells up-regulate the chemokine receptor CCR7, which promotes their migration to the boundary between the B cell-rich follicles and the T cell zones (1). Ag-activated T cells also move to this T:B border region, thus favoring the formation of cognate interactions that drive B cell proliferation.

To neutralize foreign Ag, B cells must differentiate into Ab-secreting plasmablasts (PBs) and plasma cells (PCs). PBs, the initial proliferative stage of PC differentiation, are generated during the early phases of TD responses and localize to extrafollicular areas of secondary lymphoid tissues, such as the splenic bridging channels defined by the border of the T cell zone (or periarteriolar lymphoid sheath (PALS)) and the red pulp. Migration of PBs to these extrafollicular locales is thought to be due to CXCR4-mediated chemotaxis toward CXCL12 produced in the splenic red pulp combined with the loss of CXCR5-mediated attraction toward follicular CXCL13 (2). PBs in extrafollicular foci undergo transient proliferative expansion, leading to generation of short-lived PCs. Extrafollicular foci, and thus the initial Ab response to TD Ags, last for several days only. Nevertheless, their production of unmutated Abs early in the response can be critical for the neutralization of rapidly dividing pathogens such as viruses (3). The transient nature of the TD extrafollicular response and its similarity to B cell responses to type II T-independent Ags have led to the theory that the extrafollicular expansion of PBs occurs without direct input from Th cells (4). However, the recent identification of extrafollicular, IL-21-producing, Th cells that drive IgG production by chronic autoreactive PCs (5) raises the possibility that similar T cells may also play a role in driving extrafollicular PB responses against foreign Ags.

Responding B cells can also migrate to the follicular regions of secondary lymphoid tissues and form germinal centers (GCs), in which they undergo somatic hypermutation of their Ig V region genes. This process is driven by cognate interactions with small numbers of Th follicular (T_{FH}) cells present within the GC (6). B cells that acquire increased affinity for Ag preferentially survive within the GC and subsequently differentiate into long-lived PCs or memory B cells, both of which contribute to long-term immunity. Early memory B cells can also be generated independently of the GC response and, unlike early PBs and GC B cells, can migrate into the blood and to distal lymphoid tissues

*Immunology Program, Garvan Institute of Medical Research, Darlinghurst, Australia; and †St. Vincent's Clinical School, University of New South Wales, Sydney, New South Wales, Australia

Received for publication May 29, 2009. Accepted for publication June 26, 2009.

The costs of publication of this article were defrayed in part by the payment of page charges. This article must therefore be hereby marked *advertisement* in accordance with 18 U.S.C. Section 1734 solely to indicate this fact.

[1] This work was supported by Program Grant 427620 from the National Health and Medical Research Council of Australia. R.B. was supported by a Senior Research Fellowship, and D.G. by a Biomedical Research Fellowship from the National Health and Medical Research Council of Australia.

[2] Address correspondence and reprint requests to Dr. Robert Brink, Garvan Institute of Medical Research, 384 Victoria Street, Darlinghurst NSW 2010, Australia. E-mail address: r.brink@garvan.org.au

[3] Abbreviations used in this paper: TD, T dependent; GC, germinal center; HEL, hen egg lysozyme; PALS, periarteriolar lymphoid sheath; PB, plasmablast; PC, plasma cell; T_{FH}, Th follicular.

www.jimmunol.org/cgi/doi/10.4049/jimmunol.0901690

(7, 8). Contrary to a commonly held belief, Ig class switch recombination is not restricted to the GC and can begin as early as 2 days after immunization with TD Ag (9, 10). Thus, class-switched (e.g., IgG^+) as well as unswitched (IgM^+) cells are present in the early PB and memory B cell responses, as well as within GCs (7, 9–11).

The ability of proliferating B cell blasts to differentiate within 1 week of immunization into three distinct responder populations (PBs, GC, and memory B cells) is evident from the analysis of endogenous responses to TD Ags. Investigation of how this complex process of multilineage differentiation is regulated, however, is hampered by the exceedingly low frequencies of responding lymphocytes present during the early stages of the response. Recently, systems based on the adoptive transfer of genetically labeled B cells with a defined BCR specificity have greatly improved the resolution of the early stages of Ag-specific B cell responses (10, 12, 13). Nevertheless, a clear picture of how early TD B cell differentiation is regulated awaits a detailed analysis of the phenotypic and migrational changes that occur during this time.

We have previously reported an in vivo experimental system (SW_{HEL} Ig H chain VDJ knock-in mice) that allows high-resolution analysis of TD responses mounted by B cells expressing a BCR that binds the foreign protein Ag hen egg lysozyme (HEL) (13, 14). Using this system, it was found that initial Ag affinity has a profound effect on the early PB response. Thus, whereas SW_{HEL} B cells generate good GC responses to high, intermediate, or low affinity variants of HEL, the PB response is specifically reduced when initial Ag affinity is low (11). However, the mechanism by which Ag affinity regulates the early PB response remains unclear.

To clarify the steps in early PB differentiation and the factors that regulate this process, we conducted a detailed kinetic analysis of the first 6 days of a TD response mounted by SW_{HEL} anti-HEL B cells. The picture to emerge was one of initial proliferative expansion of undifferentiated B cell blasts, followed by a dynamic phase of multilineage differentiation, including the generation of PBs secreting anti-HEL Abs of five different Ig subclasses. Our data indicate that Ag affinity is a critical regulator of the expansion rather than the differentiation of PBs, and that this effect is particularly pronounced on class-switched (IgG^+) as opposed to unswitched PBs (IgM^+). Although direct involvement of extrafollicular Th cells is possible, early PBs were shown to lack IL-21R, and thus, are unlikely to be directly influenced by T cell-derived IL-21.

Materials and Methods

Mice and adoptive transfers

SW_{HEL} mice (14), *Blimp*^{gfp} reporter mice (15), and Thy1.1 congenic OT-II TCR transgenic mice (16) were bred and housed in specific pathogen-free conditions in the Garvan Institute Biological Testing Facility. Wild-type and SJL-Ptprca (CD45.1 congenic) C57BL/6 mice were purchased from the Animal Resources Centre. Experiments were approved by the Garvan Institute/St. Vincent's Animal Experimentation Ethics Committee. Production of rHEL proteins, their conjugation to SRBCs, and adoptive transfer procedures have been described (11). In experiments directly comparing responses with $HEL^{2\times}$-SRBC and $HEL^{3\times}$-SRBC, surface densities of $HEL^{2\times}$ and $HEL^{3\times}$ were confirmed to differ by <25% by flow cytometric analysis of conjugated SRBCs using HyHEL9 Alexa Fluor 647 (11). For collaborative responses between SW_{HEL} B cells and OT-II T cells, HEL was chemically conjugated to $OVA_{323–339}$ peptide (CGGISQAVHAA HAEINEAGR) using the cross-linking agent succinimidyl-6-[β-maleimidopropionamido]hexanoate (Pierce). A mixture of spleen cells from SW_{HEL} and OT-II mice containing 3×10^4 HEL-binding B cells and 3×10^4 $V\alpha2^+$ $CD4^+$ OT-II T cells was injected i.v. into recipient mice together with 30 μg of HEL-$OVA_{323–339}$ conjugate. Recipient mice were also immunized i.p. with 100 μg of OVA (Sigma-Aldrich) in Alum (Pierce) on the day of transfer.

Abs and reagents for flow cytometry

The following mAbs were purchased from BD Biosciences: anti-CD45R/B220 PE, anti-Pacific Blue (RA3-6B2), anti-IgG1 biotin (A85-1), anti-IgG2a/c biotin (R19-15), anti-IgG2b biotin (R12-3), anti-IgG3 (R40-82), anti-κ-biotin (187.1), anti-IgD FITC (11-26c.2a), anti-IgM^b PE (AF6-78), anti-CD16/CD32 (2.4G2), anti-CD45.2 FITC (104), anti-CD184/CXCR4 biotin (2B11), anti-CXCR5 biotin (2G8), anti-Thy1.1 biotin (OX-7), and streptavidin-PE. The following mAbs were purchased from eBiosciences: anti-CD45.1 PE/Cy7 (A20), anti-CD45.2 PerCP/Cy5.5 (104), anti-CCR7 biotin (4B12), anti-CD38 PE (90), anti-CD3 biotin (500A2), and anti-IL-21R biotin (eBio4A9). Anti-IgD Alexa Fluor 647 was purchased from BioLegend (11-26c.2a). Streptavidin-Pacific Blue was purchased from Invitrogen Molecular Probes, and conjugation to Alexa Fluor 647 was performed using the Alexa Fluor 647 mAb labeling kit, according to manufacturer's instructions. Wild-type HEL was purchased from Sigma-Aldrich.

Flow cytometry

Cell suspensions from spleen and mesenteric lymph node were prepared, RBC were lysed, and FcRs were blocked with unlabeled anti-CD16/32 before staining. To detect HEL-binding cells, cells were stained with saturating levels of HEL (200 ng/ml), followed by HyHEL9 Alexa Fluor 647. Anti-IgG and anti-IgM stains were followed by 5% mouse serum before staining for other surface molecules. Cells were filtered using 35 μm filter round-bottom FACS tubes (BD Biosciences) immediately before data acquisition on either BD LSR II or FACSCanto analyzers. For annexin V-binding assays, cells were transferred into 5-ml FACS tubes and washed twice in cold PBS, washed in binding buffer, and stained with annexin V-FITC (BD Biosciences), according to manufacturer's instructions. Cytometer files acquired on Diva software (BD Biosciences) were analyzed with FlowJo software (TreeStar). Approximately 2.5×10^6 events were collected per sample. All presented data are representative of two to three experiments.

ELISA

Serum levels of anti-HEL Abs of the various Ig subclasses were measured by ELISA, as previously described (13, 14). Plates were coated with HEL (Sigma-Aldrich), and bound serum Ab detected using the same Ig H chain isotype-specific secondary Abs used for flow cytometry. Ab levels for each class of Ig were quantitated against rHyHEL10 standards (13, 14).

BrdU labeling

Mice were injected i.v. with 2.5 mg of BrdU (in 250 μl of PBS) and sacrificed 60 min later. Spleen cells were stained for surface molecules and then fixed, permeabilized, and stained with anti-BrdU FITC using the BrdU Flow Kit (BD Biosciences), according to manufacturer's instructions.

Immunofluorescence histology

Sections (6–7 μm) were cut using a Leica CM1900 cryostat, fixed in acetone, and blocked with 30% normal horse serum. To stain HEL-binding cells, sections were incubated with 200 ng/ml HEL (Sigma-Aldrich), polyclonal rabbit anti-HEL sera, and anti-rabbit IgG Cy5 (Jackson ImmunoResearch Laboratories). T cells were stained with anti-CD3 biotin (eBiosciences; 500A2), streptavidin Alexa Fluor 350 (Molecular Probes), and follicular B cells with anti-IgD FITC (BD Biosciences; 11-26c.2a). For collaborative responses between SW_{HEL} B cells and OT-II T cells, HEL-binding cells were detected as above, except using anti-rabbit IgG FITC (Jackson ImmunoResearch Laboratories), follicular B cells stained with anti-IgD Alexa Fluor 647 (BioLegend; 11-26c.2a), OT-II transgenic T cells detected with anti-Thy1.1 biotin (BD Biosciences; OX-7), and a Cy3-tyramide staining kit (PerkinElmer). Slides were analyzed with a Zeiss Axiovert 200M microscope using a ×10 objective and Adobe Photoshop software.

Results

Visualizing early TD B cell responses using SW_{HEL} mice

SW_{HEL} mice carry the specificity of the HyHEL10 anti-HEL mAb on 10–20% of their B cells and undergo normal Ig class switching and somatic hypermutation (13, 14). To track TD responses made by anti-HEL SW_{HEL} B cells, unmanipulated SW_{HEL} spleen cells containing 3×10^4 HEL-binding B cells are injected i.v. into CD45.1 congenic C57BL/6 recipient mice along with 2×10^8 SRBCs conjugated to HEL (13, 17). For parts of this study, reliable visualization of the very earliest phases of the response (days

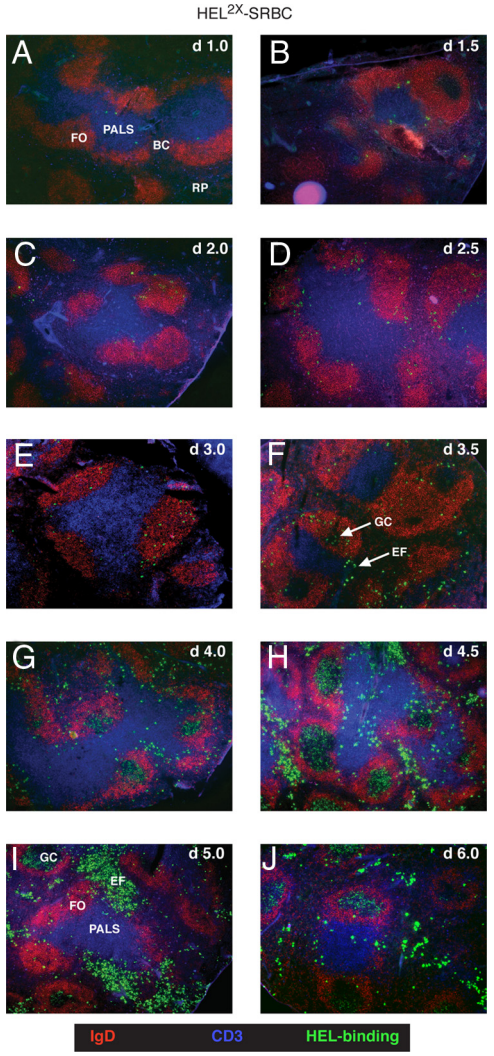

FIGURE 1. Splenic migration of SW_{HEL} B cells from day 1.0 to 6.0 of their response to $HEL^{2\times}$-SRBC. A total of 1.5×10^5 (*A–D*) or 3.0×10^4 (*E* and *F*) anti-HEL SW_{HEL} B cells was adoptively transferred and challenged with $HEL^{2\times}$-SRBC. Spleens were harvested at the indicated time points, and sections were stained for HEL-binding B cells (green), IgD (red), and CD3 (blue). SW_{HEL} responders migrate to the outer $CD3^+$ PALS by day 1.0 (*A*) and localize to the T:B border by day 1.5 (*B*). Over days 2.0–3.0 (*C–E*), SW_{HEL} B cells undergo proliferative expansion and move into the IgD^+ B cell follicle (FO). Subsequent migration into early GCs and into bridging channels (BC) to form extrafollicular foci (EF) occurs on day 3.5 (*F*). GC responses persist, whereas the EF response peaks at day 5.0 and then wanes (*G–J*).

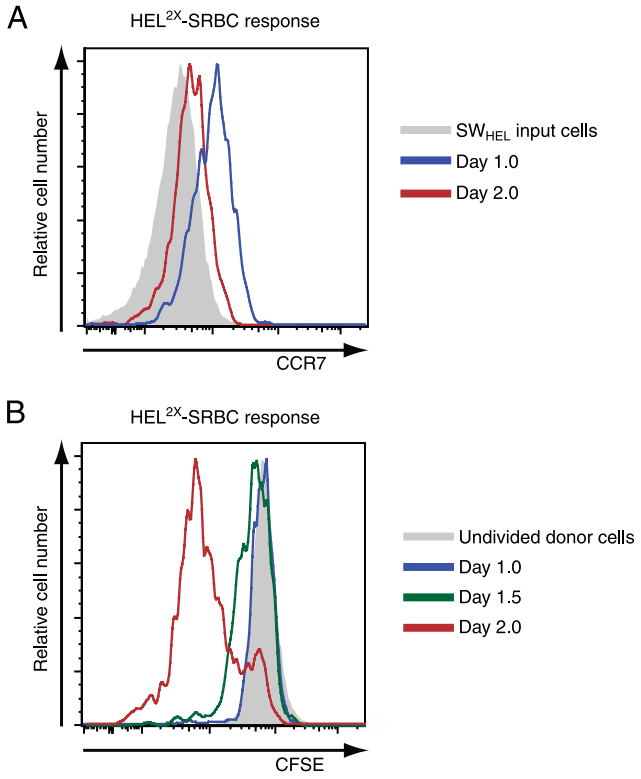

FIGURE 2. Early B cell proliferation and transient CCR7 up-regulation are independent of initial Ag affinity. *A*, A total of 1.5×10^5 anti-HEL SW_{HEL} spleen cells was challenged in adoptive transfer with $HEL^{2\times}$-SRBC, and histograms representing staining for CCR7 on donor-derived HEL-binding B cells on days 1.0 and 2.0 overlaid. Gray-filled histogram represents the expression of CCR7 on donor anti-HEL SW_{HEL} B cells before transfer. *B*, SW_{HEL} spleen cells were labeled with CFSE and 1.5×10^5 anti-HEL SW_{HEL} B cells challenged in adoptive transfer with $HEL^{2\times}$-SRBC. Recipient spleens were harvested at days 1.0, 1.5, and 2.0, and stained for flow cytometric analysis, and the CFSE fluorescence histograms of donor-derived HEL-binding B cells overlaid. Gray-filled histogram corresponds to non-HEL-binding donor cells and indicates CFSE fluorescence of undivided lymphocytes. Cell division is indicated by decreasing CFSE fluorescence.

1.0–2.5) necessitated injection of mice with increased numbers (1.5×10^5) of anti-HEL SW_{HEL} B cells. To compare the effect of initial Ag affinity on early TD B cell responses, recipient mice were challenged with SRBCs conjugated to mutant HEL proteins that bind the SW_{HEL} BCR with either intermediate affinity (8×10^7 M^{-1}; $HEL^{2\times}$) or low affinity (1.5×10^6 M^{-1}; $HEL^{3\times}$) (11). Initially, the changes in B cell migration, differentiation, and phenotype that occur during the early phases of a TD response were analyzed following challenge of SW_{HEL} B cells with the intermediate affinity Ag, $HEL^{2\times}$-SRBC.

Early B cell proliferation within the primary B cell follicle

After 24 h (day 1.0), SW_{HEL} B cells exposed to $HEL^{2\times}$-SRBC Ag were detected in the peripheral areas of the PALS, proximal to the B cell follicle (Fig. 1*A*) and showed up-regulation of cell surface CCR7 (Fig. 2*A*). At this point, SW_{HEL} B cells had commenced DNA synthesis (data not shown), but remained undivided, with cellular proliferation not evident until 12 h later (day 1.5; Fig. 2*B*). By day 2.0, almost all donor anti-HEL SW_{HEL} B cells had divided at least once, with most cells having divided at least three times in the previous 24 h (Fig. 2*B*). Rapid proliferation of SW_{HEL} B cells continued for at least the next 48 h, as evidenced by ongoing dilution of CFSE (data not shown) and accumulation of anti-HEL B cells (Fig. 1). This major proliferative expansion of the responding B cells took place primarily within the follicle. Thus, between days 1.5 and 2.0, responding B cells began to migrate into the primary follicle (Fig. 1*C*) coincident with the waning of cell surface CCR7 expression (Fig. 2*A*). By day 2.5, many responding B cells were located in the peripheral areas of the follicle, in some cases close to the bridging channel regions where the PALS meets the red pulp (Fig. 1*D*). On day 3.0, responding B cells continued to proliferate within the follicle, but had not yet formed GCs (Fig. 1*E*). This pattern of follicular proliferation of early TD B cell blasts before GC formation was also identified in a recently published study (18).

GC and extrafollicular migration occurs between days 3.0 and 4.0

On day 3.5, most SW_{HEL} B cells continued to localize among the endogenous IgD^+ cells of the B cell follicle. Some, however, had

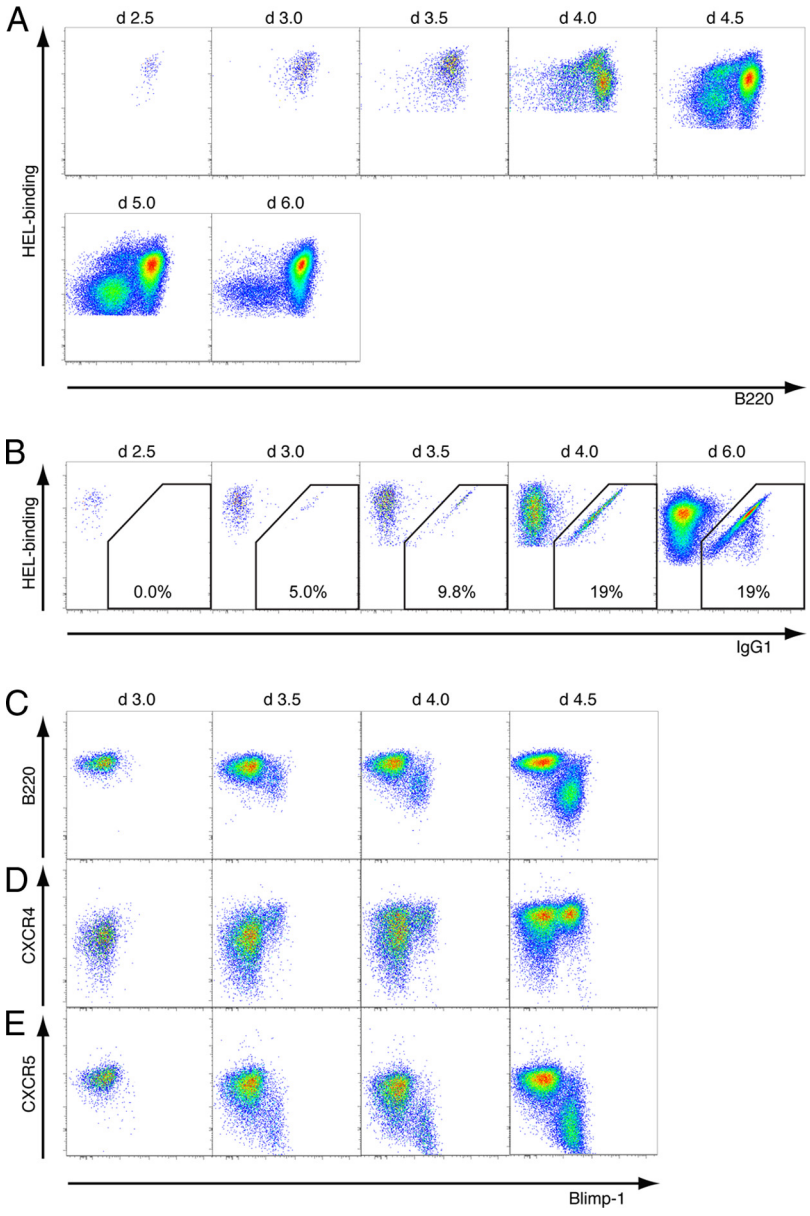

FIGURE 3. Flow cytometric time course of the response of SW_{HEL} B cells to $HEL^{2\times}$-SRBC. *A*, Responding SW_{HEL} B cells were identified by flow cytometry every 12 h from days 2.5 to 6.0. Histograms represent data obtained from equivalent numbers of recipient spleen cells (5×10^6) and so reflect the relative frequencies of responding SW_{HEL} B cells. Note the increasing frequency and phenotypic changes with regard to B220 and BCR (HEL-binding) expression. *B*, As for *A*, except showing IgG1 class switching on responding SW_{HEL} B cells. *C–E*, Spleen cells from SW_{HEL}-*Blimp*$^{gfp/+}$ donor mice were adoptively transferred, challenged with $HEL^{2\times}$-SRBC, and analyzed by FACS. Data represent HEL-binding donor-derived SW_{HEL} cells. Early Blimp-1^+ (GFP^+) PBs can be first seen between days 3.0 and 3.5 before down-regulation of B220 between days 4.0 and 4.5. The frequency of Blimp-1^+ cells within the responding populations at each time point was 1.2% (day 3.0), 9.4% (day 3.5), 16.7% (day 4.0), and 30.9% (day 4.5). *C*, CXCR4 is up-regulated on all SW_{HEL} responders between days 3.0 and 3.5 (*D*). CXCR5 is down-regulated on Blimp-1^+ PBs, but maintained on Blimp-1^- responders (*E*).

migrated into newly formed IgD^- areas of the follicle proximal to the T cell zone (Fig. 1*F*). These areas represented nascent GCs, as indicated by their staining for GL7 (data not shown). In addition, some responding B cells had left the follicle altogether and localized in the extrafollicular bridging channels and red pulp (Fig. 1*F*). By day 4.0, the shift of responding B cells into GCs and extrafollicular areas was almost complete, with very few remaining in the IgD^+ areas of the follicle (Fig. 1*G*). This pattern was maintained throughout days 4.5 and 5.0 of the response to $HEL^{2\times}$-SRBC, with the numbers of responding SW_{HEL} B cells in both areas expanding noticeably over this period (Fig. 1, *H* and *I*). By day 6.0, however, a dramatic decrease in the numbers of extrafollicular HEL-binding cells had occurred, whereas the GC response persisted (Fig. 1*J*). The migration, large size, bright intracellular staining, and response kinetics of the extrafollicular HEL-binding population were typical for a primary TD extrafollicular plasmablast response (4).

B cell blasts undergo dynamic phenotypic changes from days 3.0 to 4.0

Having established the pattern of migration of SW_{HEL} B cells during their response to $HEL^{2\times}$-SRBC, we next sought to identify the associated changes in their cell surface phenotype. To do this, recipient spleens were subjected to six-color flow cytometric analysis in which the donor SW_{HEL} B cells were identified as $CD45.2^+$, $CD45.1^-$, HEL-binding cells (17). Our initial analysis focused on the changes in expression of the B220 isoform of CD45 and of the BCR (HEL binding) over the course of the response. Proliferating B cell blasts were present at low frequencies on day 2.5 of the response (0.002–0.005% of total splenocytes) and exhibited a uniform $B220^{high}$, BCR^{high} phenotype (Fig. 3*A*). At this stage, virtually all the responding B cells were uniquely IgM^+ because they had down-regulated surface IgD, but had not yet commenced Ig class switching (data not shown and Fig. 3*B*). This phenotype was largely maintained on day 3.0, the major changes being a significant expansion in the numbers of responding SW_{HEL} B cells (Fig. 3*A*) and the appearance of the first class-switched B cells (Fig. 3*B*). This phase of proliferative expansion and initiation of class switching occurred within the primary follicle (Fig. 1, *D* and *E*).

The relatively undifferentiated $B220^{high}$, BCR^{high} cells present on day 3.0 were found to undergo profound phenotypic changes over the subsequent 24 h of the response. Cells expressing reduced

levels of BCR and/or B220 became apparent between days 3.0 and 3.5 (Fig. 3*A*) coincident with the first histological evidence of responding SW_{HEL} B cells moving into extrafollicular and GC niches (Fig. 1*F*). Distinct $B220^{high}$, BCR^{low}, and $B220^{low}$ populations were clearly apparent by day 4.0, reflecting the prominent GC and extrafollicular populations evident by histological analysis at this time point (Fig. 1*G*). The subsequent accumulation of $B220^{high}$, BCR^{low} GC phenotype B cells (Fig. 3*A*) mirrored the expansion of GCs previously detected by histology (Fig. 1), whereas the expansion and then rapid disappearance of $B220^{low}$ cells (Fig. 3*A*) were consistent with the histological documentation of the extrafollicular PB response (Fig. 1). Confirmation that the $B220^{low}$ cells derived from the SW_{HEL} donor B cells were of the PB/PC lineage was obtained by analyzing the response of SW_{HEL}-$Blimp^{gfp/+}$ B cells (15, 19) to $HEL^{2\times}$-SRBC. Thus, although *Blimp-1* (GFP) expression was initially observed on $B220^{high}$ cells from days 3.0 to 3.5 of the response, all $B220^{low}$ cells subsequently expressed this marker of PB/PC commitment. $B220^{high}$ cells, in contrast, were almost exclusively GFP^- by day 4.5 of the response (Fig. 3*C*), and so corresponded principally to the GC B cell population.

Coordinated shifts in CXCR4 and CXCR5 expression during PB differentiation

The ability to identify early, committed PBs during the response of SW_{HEL}-$Blimp^{gfp/+}$ B cells provided the opportunity to investigate their cell surface phenotype in more detail. CXCR4 and CXCR5 are critical regulators of B cell migration, and whereas mature GC B cells and PCs are known to be $CXCR4^{high}$, $CXCR5^{high}$ and $CXCR4^{high}$, $CXCR5^{low}$, respectively (2, 20), the regulation of these chemokine receptors during early differentiation has not been characterized. Expression of CXCR4 was generally low at day 3.0, but rapidly increased on virtually all responding B cells and was particularly high on early $Blimp^{gfp}$-expressing PBs (Fig. 3*D*). Expression of CXCR5 was uniformly high on the follicular blasts present on day 3.0, but was specifically lost from PBs in virtual synchrony with their expression of the $Blimp^{gfp}$ locus (Fig. 3*E*). Thus, the $CXCR4^{low}$, $CXCR5^{high}$ follicular B cell blasts present on day 3.0 of the response differentiated primarily into $CXCR4^{high}$, $CXCR5^{high}$ GC B cells or $CXCR4^{high}$, $CXCR5^{low}$ extrafollicular PBs over the ensuing 24 h.

Early production of unmutated $B220^{high}$, BCR^{high} memory B cells

Although it was clear that GC B cells and PBs partitioned, respectively, into the $B220^{high}$ and BCR^{low} compartments of the response by day 5.0, it was also apparent that both subsets exhibited significant heterogeneity of BCR expression (HEL binding). Thus, both the $B220^{high}$ and $B220^{low}$ populations were comprised of distinct BCR^{high} and BCR^{low} subsets (Fig. 4*A*). The significance of these subsets was investigated further.

Although the majority of $B220^{high}$ cells present on day 5.0 of the response of SW_{HEL} B cells to $HEL^{2\times}$-SRBC expressed relatively low levels of surface BCR, a lower frequency population of $B220^{high}$, BCR^{high} cells was also reproducibly generated (Fig. 4*A*). Most of these cells had not undergone Ig class switching (Fig. 4*C*), expressed low levels of the GC markers Fas and GL7 (data not shown), and were uniformly high for CD38, a marker present on memory, but not GC B cells in mouse (Fig. 4*B*) (21). In contrast to the $B220^{high}$, BCR^{low} population, virtually no $B220^{high}$, BCR^{high} cells were in active cell cycle, and many retained detectable levels of intracellular CFSE when originally derived from CFSE-labeled SW_{HEL} B cells (Fig. 4*B*). These data indicate that $B220^{high}$, BCR^{high} cells have participated in, but exited from the response, and thus are not GC B cells, but early, Ag-experienced, memory B cells. Consistent with this proposition, extensive somatic hypermutation of the SW_{HEL} H chain V region gene was found in the $B220^{high}$, BCR^{low} (17 of 25 clones), but not the $B220^{high}$, BCR^{high} (0 of 22 clones) population on day 5.0 of the response. In addition, $B220^{high}$, BCR^{high} cells, but not $B220^{high}$, BCR^{low} cells generated from responses to $HEL^{2\times}$-SRBC and $HEL^{3\times}$-SRBC were found in distal lymph nodes (data not shown). This putative population of early memory B cells therefore shares many of the characteristics of early memory B cell population characterized in endogenous responses to nitrophenyl phosphate-keyhole limpet hemocyanin (7). These $B220^{high}$, BCR^{high} early memory B cells were $CXCR5^{high}$, but expressed low levels of CXCR4 compared with the $B220^{high}$, BCR^{low} GC B cell population (data not shown).

IgM^+ PBs express 5- to 10-fold higher levels of BCR than IgG^+ PBs

The $B220^{low}$ cells of the PB/PC lineage generated in response to $HEL^{2\times}$-SRBC could also be resolved into those with high and low BCR levels (Figs. 3*A* and 4*A*). Analysis of Ig isotype expression indicated that unswitched (IgM^+) PBs belonged exclusively to the BCR^{high} population, whereas IgG1-switched PBs were entirely BCR^{low} (Fig. 4*C*). Thus, $IgG1^+$ PBs expressed 5- to 10-fold lower levels of BCR compared with IgM^+ PBs. This phenomenon was specific for the PB lineage because IgM^+ and $IgG1^+$ GC B cells ($B220^{high}$, BCR^{low}) did not vary significantly in their levels of BCR expression (Fig. 4*C*).

Although $IgG1^+$ PBs clearly partitioned to the $B220^{low}$, BCR^{low} fraction of the PB compartment, it was clear that they did not account for all of the responding cells with this phenotype (Fig. 4*C*). To determine whether the response of SW_{HEL} B cells to $HEL^{2\times}$-SRBC involved switching to other classes of Ig, responding B cells were analyzed on day 5.0 for surface expression of all downstream Ig H chain isotypes. This analysis did not reveal any IgE^+ or IgA^+ PBs (data not shown), but did indicate the presence of significant numbers of PBs expressing each of the IgG subclasses (Fig. 4*D*). Thus, $IgG3^+$, $IgG1^+$, $IgG2b^+$, and $IgG2c^+$ cells were all present in the PB compartment on day 5.0, at frequencies typically ranging from 5 to 10% of total PBs in the case of IgG3 to 30–40% for IgG1. All IgG^+ plasmablasts exhibited a similar $B220^{low}$, BCR^{low} phenotype (Fig. 4*D*) and made contributions to the early anti-HEL serum Ab response (Fig. 5*A*) approximately in proportion to their relative in vivo frequencies. Importantly, these class-switched PB responses were all shown to require expression of CD40 (TNFRSF5) by donor SW_{HEL} B cells (Fig. 5*B*), confirming that they were indeed generated as part of a TD Ab response.

PBs differentiate and migrate normally, but fail to expand in response to low affinity Ag

The analyses described up to this point of the study have defined in detail the migratory and phenotypic changes that occur during the earliest stages of the TD response of SW_{HEL} B cells to the intermediate affinity Ag $HEL^{2\times}$-SRBC. The next step was to carry out a parallel analysis of the early response to the low affinity TD Ag $HEL^{3\times}$-SRBC, the major objective being to identify the reason for the reduced PB and early Ab responses that are generated in response to this Ag (11).

Histological analysis of the early phase of the response to $HEL^{3\times}$-SRBC revealed a pattern of migration and expansion very similar to that observed for $HEL^{2\times}$-SRBC (data not shown). This was true until ~day 4.5 of the response, in which similar frequencies of HEL-binding GC B cells and extrafollicular PBs could be

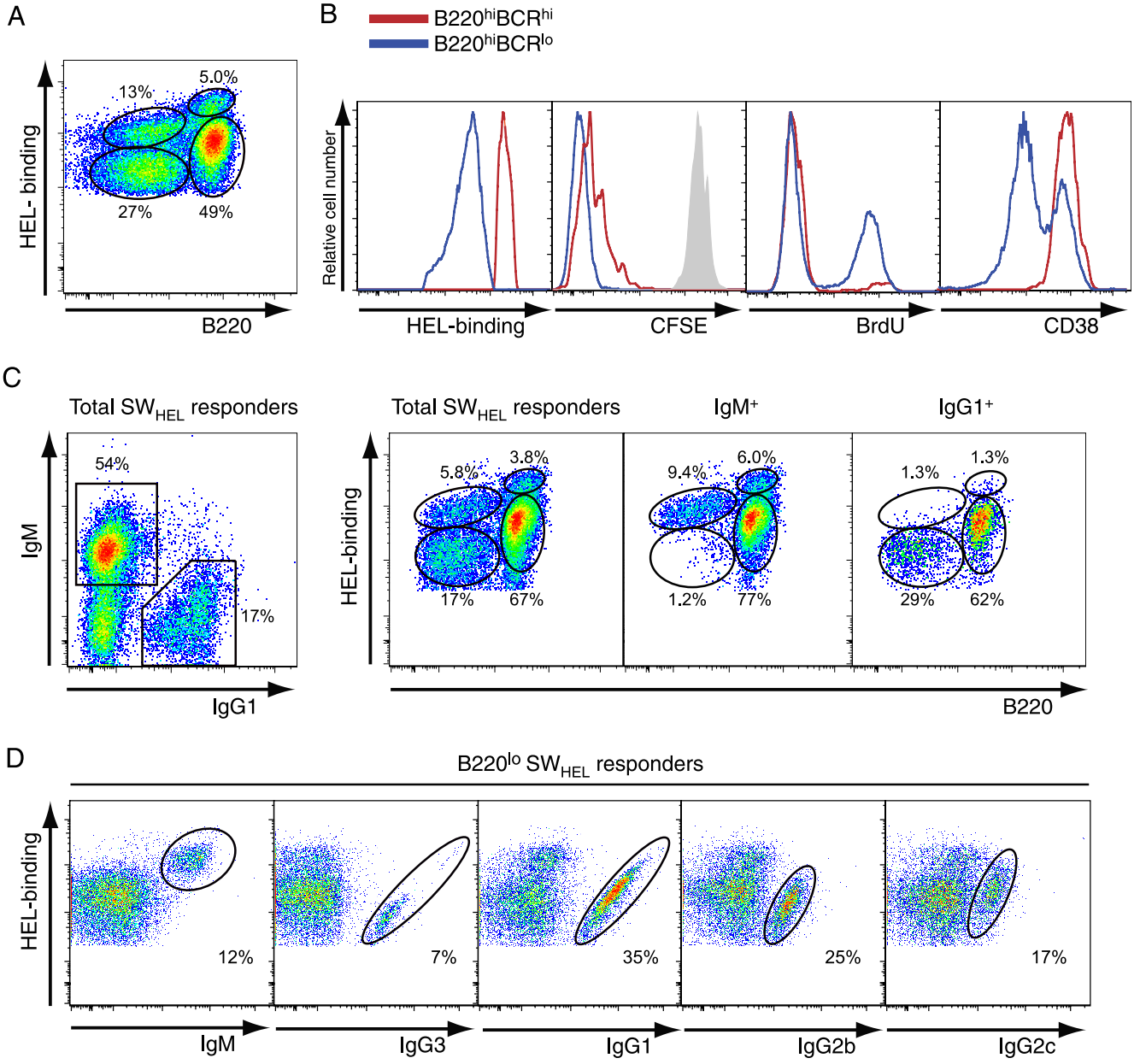

FIGURE 4. Identification of BCR^{high} and BCR^{low} components of the response to HEL$^{2\times}$-SRBC. B cells from SW$_{HEL}$ or SW$_{HEL}$-*Blimp*$^{gfp/+}$ donor mice were challenged with HEL$^{2\times}$-SRBC, and spleens were harvested for flow cytometric analysis on day 5.0. Unless otherwise stated, all plots represent data from donor-derived (CD45.2$^+$, CD45.1$^-$) HEL-binding cells (=total SW$_{HEL}$ responders). *A*, Cells expressing high and low levels of BCR (HEL binding) are present in both the B220^{high} and B220^{low} (PB/PC) populations. *B*, Comparison of B220^{high}, BCR^{high} and B220^{high}, BCR^{low} responding populations. Overlaid histograms correspond to fluorescence data from B220^{high}, BCR^{high} and B220^{high}, BCR^{low} cells identified using the gates shown in *A*. For CFSE analysis, donor SW$_{HEL}$ spleen cells were labeled with CFSE before transfer, and the gray histogram represents undivided donor B cells. For BrdU incorporation analysis, recipient mice were injected with BrdU 1 h before sacrifice. *C*, Switched and unswitched PBs are BCR^{low} and BCR^{high}, respectively. BCR levels on IgM$^+$ and IgG1$^+$ responding cells were compared using the indicated gates. *D*, SW$_{HEL}$ responders were stained separately for IgM, IgG3, IgG1, IgG2b, and IgG2c, and gated on donor-derived (CD45.2$^+$, CD45.1$^-$) HEL-binding PBs (B220^{low} SW$_{HEL}$ responders), and isotype-positive cells were analyzed for HEL-binding BCR by flow cytometry.

observed in the two responses (Fig. 6, *A* and *B*). By day 5.0, however, it was apparent not only that the extrafollicular PB population had not expanded in the HEL$^{3\times}$-SRBC response, but that it had undergone a sharp decrease (Fig. 6, *C* and *D*). A specific depletion of B220^{low} PBs between days 4.5 and 5.0 of the response to HEL$^{3\times}$-SRBC was also apparent from comparison of flow cytometry profiles obtained at this phase of the response (Fig. 6*E*). These data argued, therefore, that it is not the commitment of SW$_{HEL}$ B cells to PB differentiation or indeed the extrafollicular migration of these cells that is compromised in the response to HEL$^{3\times}$-SRBC, but their subsequent extrafollicular expansion.

Increased Ag affinity preferentially promotes expansion of IgG$^+$ PBs

To obtain a more detailed picture of the regulation of individual responding populations by Ag affinity, responding SW$_{HEL}$ cells were enumerated using flow cytometry. Consistent with the histological data described previously (Fig. 6, *A–D*), the HEL$^{3\times}$-SRBC

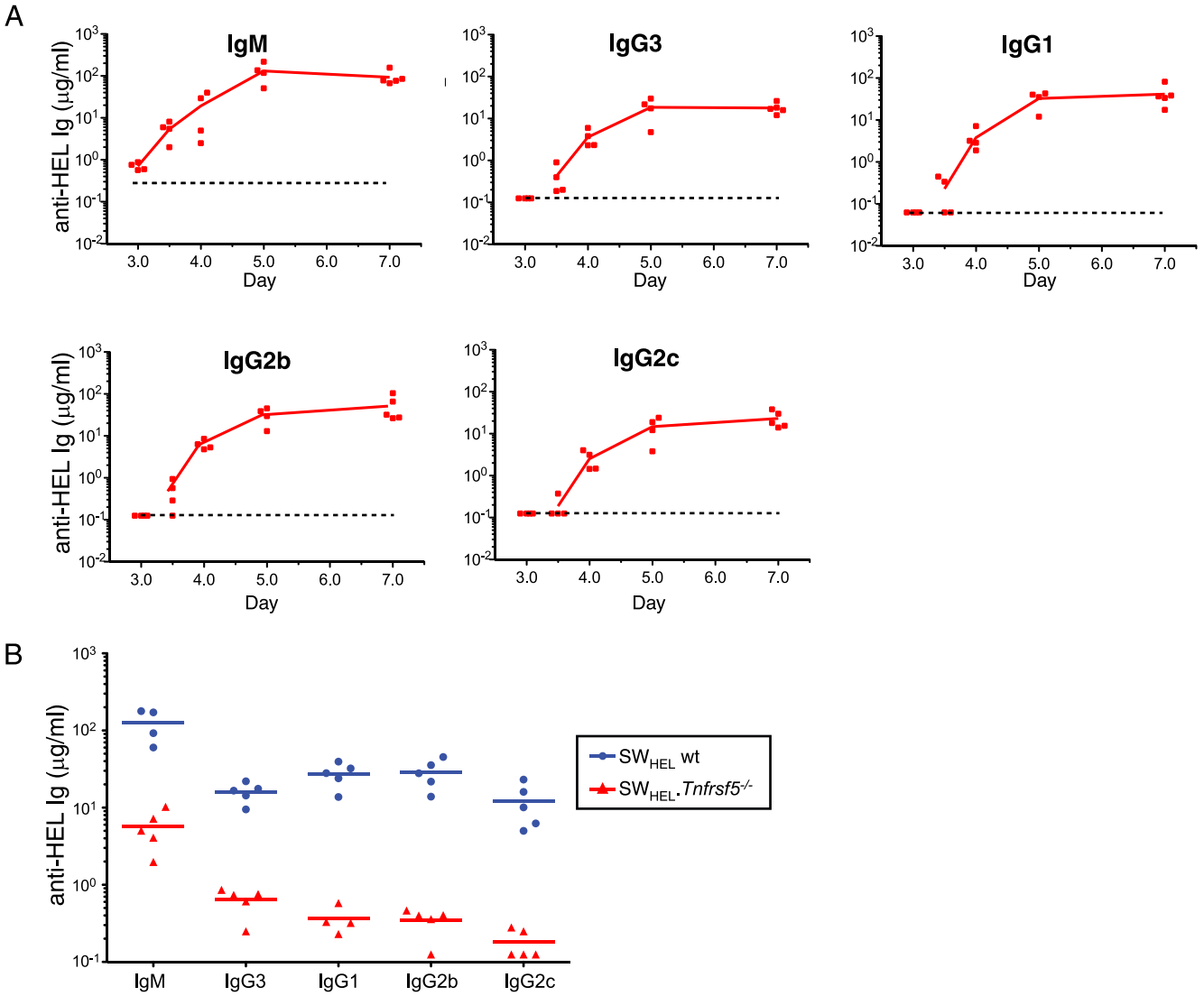

FIGURE 5. Contribution of all IgG isotypes to the early TD Ab response. SW$_{HEL}$ B cells were challenged in adoptive transfer with HEL$^{2\times}$-SRBC, and serum was collected for detection of secreted anti-HEL Ab on days 3.0, 3.5, 4.0, 5.0, and 7.0 by ELISA. *A*, Time-course analysis of serum Ab response. Dotted lines indicate limits of detection of the ELISAs based on readings from unimmunized CD45.1 congenic C57BL/6 mice. Points indicate data from individual mice, and lines connect mean levels at each time point. *B*, Wild-type and *Tnfrsf5*$^{-/-}$ (CD40-deficient) SW$_{HEL}$ B cells were challenged with HEL$^{2\times}$-SRBC in adoptive transfer, and recipient sera were analyzed on day 5.0 for anti-HEL Ab production. High-level production of all classes of Ig, but especially IgG1, IgG2b, and IgG2c, required CD40 expression by SW$_{HEL}$ B cells, and thus was TD.

response typically produced only slightly (25–35%) fewer GC B cells (B220^{high}, BCR^{low}), IgM$^+$ PBs (B220^{low}, BCR^{high}), and IgG$^+$ PBs (B220^{low}, BCR^{low}) by day 4.5 compared with the response to HEL$^{2\times}$-SRBC (Fig. 7*A*). Subsequent divergence of the two responses was most obvious in the expansion of IgG$^+$ PBs. Thus, whereas the numbers of IgG$^+$ PBs increased until day 5.0 before declining in the HEL$^{2\times}$-SRBC response, the same population declined immediately after day 4.5 in the HEL$^{3\times}$-SRBC response such that the numbers of these cells were typically 80–90% lower after this point compared with the HEL$^{2\times}$-SRBC response (Fig. 7*A*). In contrast, the numbers of IgM$^+$ PBs declined rapidly in both responses after day 4.5, whereas the GC response in each case peaked between days 5.0 and 5.5 and was typically only 30–40% reduced in the HEL$^{3\times}$-SRBC response (Fig. 7*A*). Thus, the major difference between the responses to the low and intermediate affinity Ags was the failure to expand rather than generate IgG$^+$ PBs in response to the low affinity Ag HEL$^{3\times}$-SRBC. As would be predicted from these results, the levels of anti-HEL serum Abs of nearly all IgG subclasses showed large increases between days 4.5 and 6.0 of the response to HEL$^{2\times}$-SRBC, but not to HEL$^{3\times}$-SRBC (Fig. 7*B*). The anti-HEL IgM response, in contrast, did not show a parallel increase over this period of the HEL$^{2\times}$-SRBC response and represented the class of anti-HEL Ab whose overall production was least affected by Ag affinity (Fig. 7*B*).

Ag affinity regulates PB proliferation and apoptosis

To explore the basis for the failure of low affinity Ag to support more sustained expansion of IgG$^+$ PBs, we examined the rates of proliferation and apoptosis among responding subpopulations using transient BrdU incorporation and annexin V staining, respectively. On day 4.0, 40–55% of cells in all responding populations were undergoing active DNA synthesis (Fig. 7*C*). The GC B cell (B220^{high}, BCR^{low}) populations largely maintained this high rate of proliferation for the next 24 h. In contrast, the rate of proliferation among the PB populations dropped dramatically between days 4.0 and 5.0 (Fig. 7*C*). Although this was evident in all PB populations, the rate of decrease was most striking among the IgG$^+$ PBs in the HEL$^{3\times}$-SRBC response. Thus, by day 5.0, the

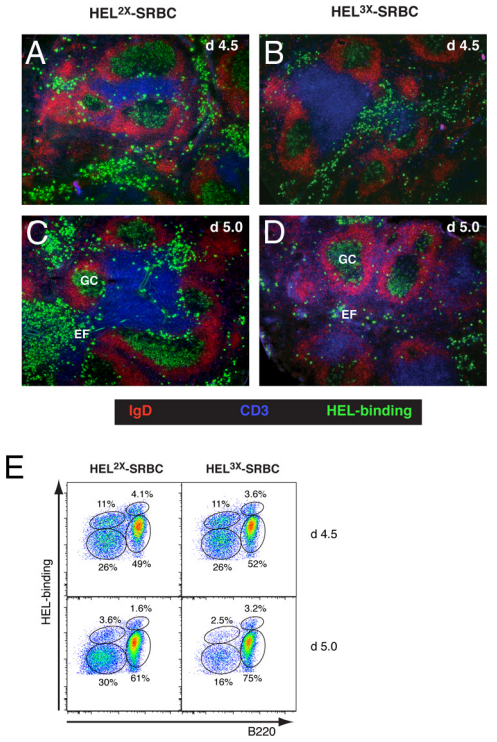

FIGURE 6. Expansion of SW_{HEL} PBs between days 4.5 and 5.0 requires sufficiently high Ag affinity. A total of 3.0×10^4 anti-HEL SW_{HEL} B cells was adoptively transferred and challenged with either $HEL^{2\times}$-SRBC or $HEL^{3\times}$-SRBC, and their migration was analyzed by immunohistology of recipient spleens, as for Fig. 1. Prominent GCs and extrafollicular foci (EF) are detected in each case at day 4.5 (*A* and *B*). This continues in the case of the $HEL^{2\times}$-SRBC response (*C*), whereas the EF response specifically and dramatically declines on day 5.0 of the response to $HEL^{3\times}$-SRBC response (*D*). *E*, Parallel flow cytometric analysis showing the specific reduction in the $B220^{low}$ PB response to $HEL^{3\times}$-SRBC.

rate of BrdU incorporation among IgG^+ PBs was twice as high in the $HEL^{2\times}$-SRBC compared with the $HEL^{3\times}$-SRBC response (Fig. 7*D*).

Because day 4.5 is the point at which the PB responses to low and intermediate affinity Ag diverged, the commitment of PBs to apoptosis at this time point was assessed by annexin V staining. Less than 1% GC B cells from either the $HEL^{2\times}$-SRBC or the $HEL^{3\times}$-SRBC response bound annexin V on day 4.5 (Fig. 7*E*). In contrast, relatively high frequencies of early PBs (4–24%) bound annexin V (Fig. 7*E*), consistent with the transient nature of these populations (Fig. 7*A*). As was observed for BrdU incorporation, the largest difference between the frequencies of annexin V-binding cells in the $HEL^{2\times}$-SRBC vs the $HEL^{3\times}$-SRBC response was among the IgG^+ PBs (3-fold higher in the $HEL^{3\times}$-SRBC response; Fig. 7*E*). Taken together, these data show that the failure of IgG^+ PBs to expand in the $HEL^{3\times}$-SRBC compared with the $HEL^{2\times}$-SRBC response is due to both a reduced rate of proliferation and a higher rate of apoptosis.

Extrafollicular PBs express class II MHC, but not IL-21R and interact with extrafollicular Th cells

Our analysis indicated that increased Ag affinity drives the expansion of PBs within the extrafollicular regions to which they migrate. Although the increased proliferation and survival responsible for this preferential expansion could be due to a number of different mechanisms, one possibility is that Ag affinity enhances interactions with a recently identified population of IL-21-producing extrafollicular Th cells (5). To test this possibility, we verified whether extrafollicular PBs generated in response to $HEL^{2\times}$-SRBC had the potential to undergo cognate interactions with Th cells and the ability to respond to IL-21. As shown in Fig. 8*A*, $B220^{low}$ PBs present at the day 5.0 peak of the response express class II MHC at levels similar to those on the $B220^{high}$ GC B cells, and thus, have the potential to present Ag to any cognate extrafollicular T cells that may be present. However, $B220^{low}$ PBs lose expression of IL-21R as they differentiate from their $B220^{high}$ precursors (Fig. 8*B*), making it very unlikely that IL-21 is directly involved in driving the expansion of these extrafollicular PBs.

To determine whether extrafollicular PBs responding to foreign Ag can interact with Th cells, we used a modified form of the SW_{HEL} adoptive transfer system in which mice also receive OT-II anti-OVA (anti-OVA) TCR transgenic T cells and are immunized with a soluble conjugate of HEL to a peptide ($OVA_{323–339}$) that is recognized by the OT-II TCR (16). This approach allows simultaneous visualization of Ag-specific B cells and $CD4^+$ T cells mounting a collaborative response in vivo. The kinetics of this response are slightly slower than the HEL-SRBC system such that GCs and extrafollicular foci do not peak until day 6.0. As expected, SW_{HEL} GC B cells and smaller numbers of OT-II T_{FH} cells were both apparent within GCs at this point (Fig. 8*C*). Strikingly, similar ratios of SW_{HEL} PBs and OT-II $CD4^+$ T cells were also detected within extrafollicular foci. Of particular significance was the fact that several direct interactions between SW_{HEL} PBs and OT-II $CD4^+$ T cells were apparent within extrafollicular foci (Fig. 8*C*). Thus, extrafollicular PBs responding to foreign Ag can indeed form cognate interactions with extrafollicular Th cells.

Discussion

In this study, we describe a detailed analysis of the proliferation, differentiation, and migration of Ag-specific B cells during their early response to TD Ag. The picture that emerged confirms a number of previous observations, including the initial up-regulation of CCR7 and T:B border migration of Ag-activated B cells (Figs. 1 and 2*A*) (1), the subsequent follicular migration and pre-GC Ig class switching by undifferentiated B cell blasts (Figs. 1 and 3*C*) (9, 10, 18), the generation of early memory B cells (Fig. 4*B*) (7), and the $CXCR4^{high}$, $CXCR5^{high}$ and $CXCR4^{high}$, $CXCR5^{low}$ phenotypes ultimately adopted by GC B cells and extrafollicular PBs, respectively (Fig. 3, *C–E*) (2, 20). Our analysis has also revealed a number of unreported features of early TD B cell responses. These include the reversal of acute CCR7 up-regulation that accompanies follicular homing of early B cell blasts (Figs. 1 and 2*A*), the synchronous multilineage differentiation of follicular B cell blasts that occurs from day 3.0 to 4.0 of the response (Figs. 1 and 3*A*), the distinct BCR phenotypes of switched and unswitched PBs (Fig. 4, *C* and *D*), and the simultaneous counterregulation of CXCR4 and CXCR5 expression that accompanies commitment to PB differentiation (Fig. 3, *D* and *E*). The SW_{HEL} system and the detailed map of early B cell differentiation it has provided should prove to be a valuable tool for understanding how different genetic and antigenic variables impact on the generation of humoral immunity.

A key aim of this study was to identify the mechanism by which the initial affinity of Ag for the BCR positively regulates early TD PB responses (11). Despite the >50-fold lower affinity of $HEL^{3\times}$ for the SW_{HEL} BCR, the responses of SW_{HEL} B cells to $HEL^{2\times}$-SRBC and $HEL^{3\times}$-SRBC were virtually identical until day 4.5. This included the generation of extrafollicular PBs identifiable both by immunohistology (Fig. 6, *A* and *B*) and flow cytometry (Figs. 6*E* and 7*A*). This result demonstrates that the initial affinity of the BCR for TD Ag, at least over this affinity range, does not significantly influence the differentiation of PBs from follicular B

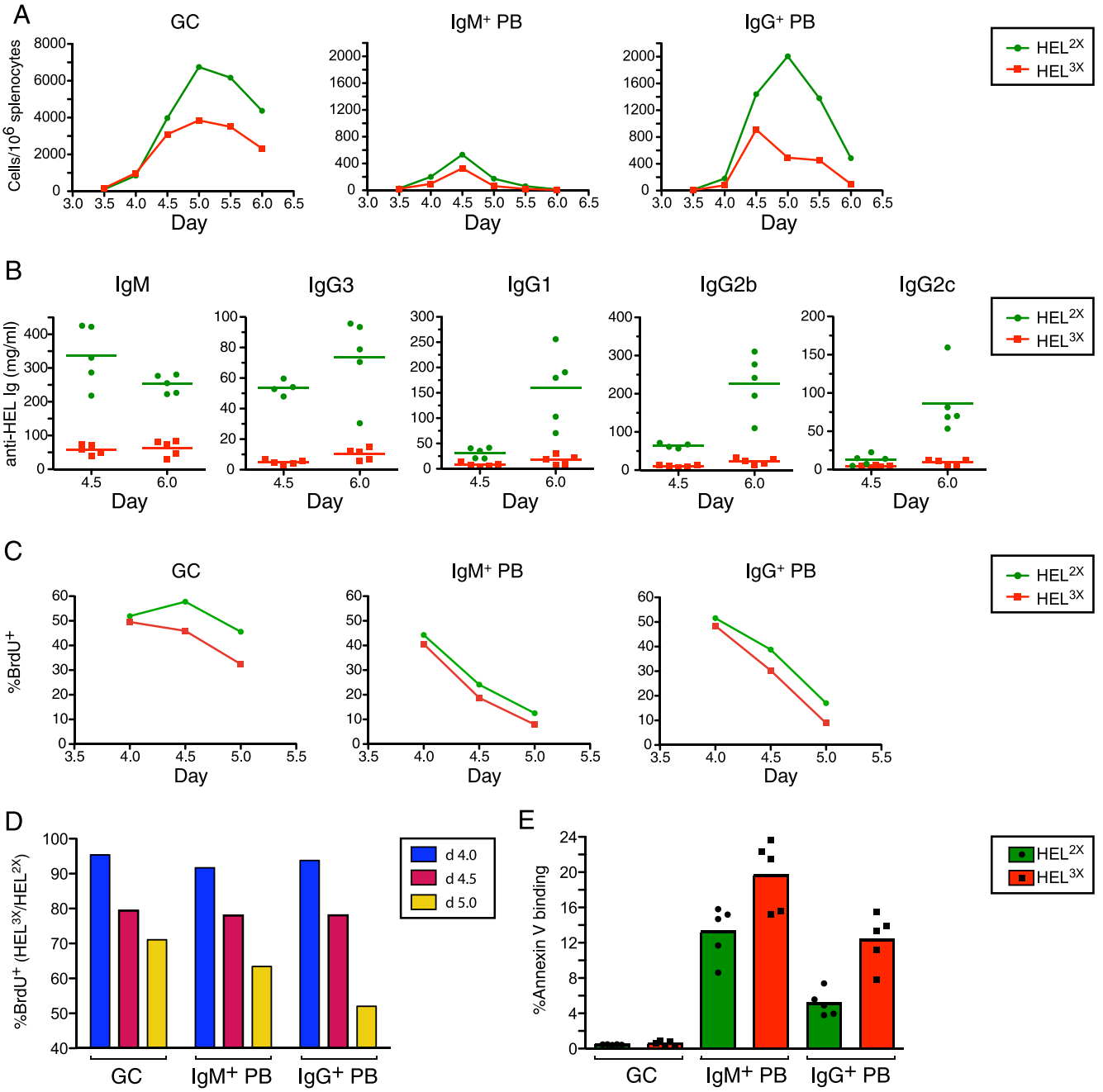

FIGURE 7. IgG$^+$ PBs preferentially expand in response to high affinity Ag due to increased proliferation and reduced apoptosis. *A*, Spleens from recipient mice were analyzed by flow cytometry every 12 h from days 3.5 to 6.0 after adoptive challenge of SW_{HEL} B cells with either HEL$^{2\times}$-SRBC or HEL$^{3\times}$-SRBC, as for Fig. 6*A*. Data represent the frequencies of GC B cells (B220^{high}, BCR^{low}), IgM$^+$ PBs (B220^{low}, BCR^{high}), and IgG$^+$ PBs (B220^{low}, BCR^{low}) in pooled spleens from three equivalently treated recipients. *B*, Sera from recipient mice challenged, as for *A*, were analyzed at days 4.5 and 6.0 of the response, and levels of the various classes of anti-HEL Ab were measured. Note the specific expansion of class-switched Ab production over this period in the HEL$^{2\times}$-SRBC, but not in the HEL$^{3\times}$-SRBC response. *C*, Donor-derived SW_{HEL} cells were assayed for active DNA synthesis (BrdU incorporation) between days 4.0 and 5.0 of the response. Spleens were harvested 1 h after BrdU injection. Data represent the fraction of BrdU$^+$ cells in the various populations analyzed, as for *A*. *D*, Data from *C* expressed as a ratio of percentage of BrdU$^+$ in the HEL$^{3\times}$-SRBC vs HEL$^{2\times}$-SRBC responses. *E*, Assessment of annexin V binding by donor-derived SW_{HEL} cells harvested on day 4.5. Subpopulations were defined, as for *A*. Points represent data from individual mice, and columns the means.

cell blasts or their extrafollicular migration. What is clearly influenced by Ag affinity, however, is the subsequent proliferative expansion of this population (Figs. 6, *C* and *D*, and 7*A*). This effect is particularly pronounced in IgG$^+$ PBs and is due to increased cell division and decreased apoptosis when Ag affinity is raised (Fig. 7, *C* and *E*).

A feature of the early stages of the responses to both HEL$^{2\times}$-SRBC and HEL$^{3\times}$-SRBC was their maintenance of relatively high BCR levels before the onset of GC and PB differentiation that occurs between days 3.0 and 4.0 (Fig. 3*A*). The fact that the effects of Ag affinity are apparent soon after this (Fig. 7*A*) is most likely not to be a coincidence, because BCR down-regulation would be expected to place increased stringency on the response in terms of the affinity of Ag required for effective BCR interactions. The preferential expansion of IgG$^+$ as opposed to IgM$^+$ PBs (Fig. 7*A*) suggests that IgG rather than IgM BCRs most efficiently mediate

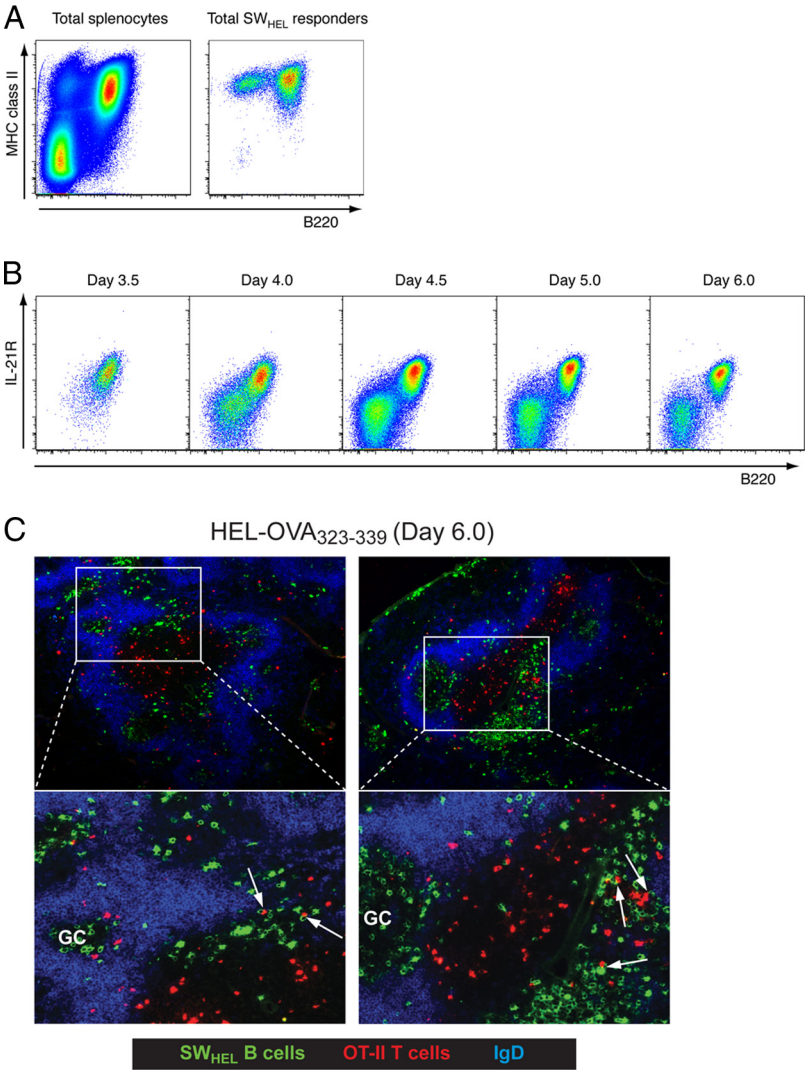

FIGURE 8. Extrafollicular PBs express class II MHC, but not IL-21R. *A*, Day 5.0 spleen analysis of SW_{HEL} responders challenged with $HEL^{2\times}$-SRBC showed the expected high MHC class II expression on GC B cells ($B220^{high}$); however, it was maintained at high levels also on early PBs ($B220^{low}$ responders). *B*, Time course analysis between days 3.5 and 6.0 of SW_{HEL} responders challenged with $HEL^{2\times}$-SRBC and stained for IL-21R expression. IL-21R expression was high on undifferentiated B cell blasts (day 3.5), but lost upon differentiation into $B220^{high}$ PBs. *C*, Histological analysis of a recipient spleen 6.0 days after cotransfer of anti-HEL SW_{HEL} B cells (green) and $Thy1.1^+$ OT-II anti-OVA $CD4^+$ T cells (red) and challenge with HEL-$OVA_{323–339}$. Follicles are stained with anti-IgD (blue). Note the presence of most OT-II T cells in the PALS, the colocalization of Ag-specific B and T cells in GCs and extrafollicular foci, and the cognate interactions between extrafollicular PBs and Th cells in the extrafollicular foci.

the Ag-dependent activities required for PB expansion, regardless of the higher BCR levels on IgM^+ PBs (Fig. 4*C*). This result corroborates earlier observations in Ig transgenic animals that indicated that the membrane-spanning regions of IgG1 as opposed to IgM promote PB expansion (22). Nevertheless, the critical BCR-mediated function that promotes PB expansion in vivo remains unclear.

The simplest role for the BCR in this regard would be to transmit to either PBs or their precursors signals that promote PB proliferation and survival. There is no fundamental requirement for BCR signals to sustain PB proliferation and survival, because B cells stimulated only with Th cell-derived stimuli such as CD40L and IL-4 produce sustained plasmablast responses (23). It could be argued, therefore, that the critical outcome of the Ag:BCR interaction in terms of PB expansion is most likely to be the facilitation of Ag presentation, and thus, effective recruitment of T cell help. It is possible that the relevant interactions with Th cells could occur before the extrafollicular migration of PBs, that is, the expansion of PBs in the bridging channels and red pulp may be driven through the inertia of signals received from Th cells within the follicle, and these may be significantly prolonged for higher affinity B cells. However, it has recently been shown that extrafollicular Th cells can drive Ab production by PCs (5). Because extrafollicular PBs retain class II MHC (Fig. 8*A*), they do have the theoretical ability to form cognate interactions with these cells. Indeed, we saw evidence of such interactions occurring between extrafollicular anti-HEL PBs and anti-OVA $CD4^+$ T cells in response to HEL-$OVA_{323–339}$ conjugate Ag (Fig. 8*C*). If extrafollicular Th cells are involved in supporting the extrafollicular PB response, their role is clearly only transient and thus stands in contrast to that of T_{FH} cells in GCs. This could be explained by the fact that, unlike GCs and PCs involved in chronic autoantibody responses such as the one in which extrafollicular Th cells were first identified (5), PBs generated in response to foreign Ag may no longer be able to access this Ag in the extrafollicular regions of secondary lymphoid tissues. In this case, they may only receive transient assistance from Th cells before their pool of peptide-MHC II complexes is exhausted. Whatever the roles of Th cells are in driving PB expansion, a direct function for IL-21 in this process seems unlikely due to the down-regulation of IL-21R expression that accompanies PB differentiation (Fig. 8*B*).

Resolution of the precise mechanism by which the Ag:BCR interaction drives PB expansion will be difficult to resolve due to the transient nature of PB expansion and the problems associated with dissociating BCR signaling from Ag presentation during this narrow window of the response. Our attempts to either neutralize Th cells using anti-CD4 Ab administration during responses to $HEL^{2\times}$-SRBC or to augment Th signals using anti-CD40 agonist Ab during responses to $HEL^{3\times}$-SRBC did not yield convincing evidence of direct Th cell involvement in PB expansion (data not

shown). However, precise activation/inactivation of Th cells at the appropriate point in the response is difficult to achieve or indeed determine. Similarly, attempts to augment BCR signaling in PBs by administering exogenous HEL during responses to $HEL^{3\times}$-SRBC did not indicate a role for these signals in driving PB expansion (data not shown). In this case, however, it is not clear that the specific nature of the BCR signal delivered to the PBs was appropriate. Because PBs generated in response to foreign Ag can form cognate interactions with extrafollicular Th cells (Fig. 8*C*), it seems likely that this newly identified population does play a prominent role in driving PB responses and perhaps mediating affinity-dependent PB expansion. Further experimentation will hopefully resolve this issue and perhaps then point toward vaccine design strategies that may enhance early Ab responses and thus provide more rapid production of protective Abs postvaccination.

Acknowledgments

We thank the staff of the Garvan Institute Biological Testing Facility for animal husbandry; Vivian Turner for mouse screening; Chris Brownlee for cell sorting; and Drs. Stuart Tangye, Tri Phan, and Alex Swarbrick for critical review of the manuscript.

Disclosures

The authors have no financial conflict of interest.

References

1. Reif, K., E. H. Ekland, L. Ohl, H. Nakano, M. Lipp, R. Forster, and J. G. Cyster. 2002. Balanced responsiveness to chemoattractants from adjacent zones determines B-cell position. *Nature* 416: 94–99.
2. Hargreaves, D. C., P. L. Hyman, T. T. Lu, V. N. Ngo, A. Bidgol, G. Suzuki, Y. R. Zou, D. R. Littman, and J. G. Cyster. 2001. A coordinated change in chemokine responsiveness guides plasma cell movements. *J. Exp. Med.* 194: 45–56.
3. Luther, S. A., I. Maillard, F. Luthi, L. Scarpellino, H. Diggelmann, and H. Acha-Orbea. 1997. Early neutralizing antibody response against mouse mammary tumor virus: critical role of viral infection and superantigen-reactive T cells. *J. Immunol.* 159: 2807–2814.
4. MacLennan, I. C., K. M. Toellner, A. F. Cunningham, K. Serre, D. M. Sze, E. Zuniga, M. C. Cook, and C. G. Vinuesa. 2003. Extrafollicular antibody responses. *Immunol. Rev.* 194: 8–18.
5. Odegard, J. M., B. R. Marks, L. D. DiPlacido, A. C. Poholek, D. H. Kono, C. Dong, R. A. Flavell, and J. Craft. 2008. ICOS-dependent extrafollicular helper T cells elicit IgG production via IL-21 in systemic autoimmunity. *J. Exp. Med.* 205: 2873–2886.
6. King, C., S. G. Tangye, and C. R. Mackay. 2008. T follicular helper (TFH) cells in normal and dysregulated immune responses. *Annu. Rev. Immunol.* 26: 741–766.
7. Blink, E. J., A. Light, A. Kallies, S. L. Nutt, P. D. Hodgkin, and D. M. Tarlinton. 2005. Early appearance of germinal center-derived memory B cells and plasma cells in blood after primary immunization. *J. Exp. Med.* 201: 545–554.
8. Inamine, A., Y. Takahashi, N. Baba, K. Miyake, T. Tokuhisa, T. Takemori, and R. Abe. 2005. Two waves of memory B-cell generation in the primary immune response. *Int. Immunol.* 17: 581–589.
9. Toellner, K. M., A. Gulbranson-Judge, D. R. Taylor, D. M. Sze, and I. C. MacLennan. 1996. Immunoglobulin switch transcript production in vivo related to the site and time of antigen-specific B cell activation. *J. Exp. Med.* 183: 2303–2312.
10. Pape, K. A., V. Kouskoff, D. Nemazee, H. L. Tang, J. G. Cyster, L. E. Tze, K. L. Hippen, T. W. Behrens, and M. K. Jenkins. 2003. Visualization of the genesis and fate of isotype-switched B cells during a primary immune response. *J. Exp. Med.* 197: 1677–1687.
11. Paus, D., T. G. Phan, T. D. Chan, S. Gardam, A. Basten, and R. Brink. 2006. Antigen recognition strength regulates the choice between extrafollicular plasma cell and germinal center B cell differentiation. *J. Exp. Med.* 203: 1081–1091.
12. Shih, T. A., E. Meffre, M. Roederer, and M. C. Nussenzweig. 2002. Role of BCR affinity in T cell dependent antibody responses in vivo. *Nat. Immunol.* 3: 570–575.
13. Phan, T. G., S. Gardam, A. Basten, and R. Brink. 2005. Altered migration, recruitment, and somatic hypermutation in the early response of marginal zone B cells to T cell-dependent antigen. *J. Immunol.* 174: 4567–4578.
14. Phan, T. G., M. Amesbury, S. Gardam, J. Crosbie, J. Hasbold, P. D. Hodgkin, A. Basten, and R. Brink. 2003. B cell receptor-independent stimuli trigger immunoglobulin (Ig) class switch recombination and production of IgG autoantibodies by anergic self-reactive B cells. *J. Exp. Med.* 197: 845–860.
15. Kallies, A., J. Hasbold, D. M. Tarlinton, W. Dietrich, L. M. Corcoran, P. D. Hodgkin, and S. L. Nutt. 2004. Plasma cell ontogeny defined by quantitative changes in blimp-1 expression. *J. Exp. Med.* 200: 967–977.
16. Barnden, M. J., J. Allison, W. R. Heath, and F. R. Carbone. 1998. Defective TCR expression in transgenic mice constructed using cDNA-based α- and β-chain genes under the control of heterologous regulatory elements. *Immunol. Cell Biol.* 76: 34–40.
17. Brink, R., T. G. Phan, D. Paus, and T. D. Chan. 2008. Visualizing the effects of antigen affinity on T-dependent B-cell differentiation. *Immunol. Cell Biol.* 86: 31–39.
18. Coffey, F., B. Alabyev, and T. Manser. 2009. Initial clonal expansion of germinal center B cells takes place at the perimeter of follicles. *Immunity* 30: 599–609.
19. Phan, T. G., D. Paus, T. D. Chan, M. L. Turner, S. L. Nutt, A. Basten, and R. Brink. 2006. High affinity germinal center B cells are actively selected into the plasma cell compartment. *J. Exp. Med.* 203: 2419–2424.
20. Allen, C. D., K. M. Ansel, C. Low, R. Lesley, H. Tamamura, N. Fujii, and J. G. Cyster. 2004. Germinal center dark and light zone organization is mediated by CXCR4 and CXCR5. *Nat. Immunol.* 5: 943–952.
21. Ridderstad, A., and D. M. Tarlinton. 1998. Kinetics of establishing the memory B cell population as revealed by CD38 expression. *J. Immunol.* 160: 4688–4695.
22. Martin, S. W., and C. C. Goodnow. 2002. Burst-enhancing role of the IgG membrane tail as a molecular determinant of memory. *Nat. Immunol.* 3: 182–188.
23. Hasbold, J., L. M. Corcoran, D. M. Tarlinton, S. G. Tangye, and P. D. Hodgkin. 2004. Evidence from the generation of immunoglobulin G-secreting cells that stochastic mechanisms regulate lymphocyte differentiation. *Nat. Immunol.* 5: 55–63.